UNIVERSITY OF CALIFORNIA, SAN DIEGO

Silicon Nanowire Compatibility Analysis with Rat Hippocampal Progenitor Cells for use in Neuroprosthetics Development

A thesis submitted in partial satisfaction of the requirements
for the degree Master of Science

in

Biology

by

Eun Kyung Joanne Lee

Committee in charge:

Professor Deli Wang, Chair
Professor Willie Claiborne Brown, Co-Chair,
Professor Milton Saier

2014

The Thesis of Eun Kyung Joanne Lee is approved and it is acceptable in quality and form for publication on microfilm and electronically:

Co-Chair

Chair

University of California, San Diego

2014

DEDICATION

This thesis is dedicated to my parents and my husband for their unconditional love and support, and to everyone who believes in me. Thank you.

TABLE OF CONTENTS

LIST OF FIGURES

ACKNOWLEDGEMENTS

First, I would like to acknowledge Dr. Deli Wang for his support as the chair of my committee and my mentor. I was extremely fortunate to be given the opportunity to further my educational pursuits under Dr. Deli Wang and I thank him for all his invaluable advises and support over the years. I thank him for the unwavering trust he has had for my work and for his compassion as my mentor. I would like to thank Dr. Willie Brown and Dr. Milton Saier for their decision to take part in my thesis committee and for offering their time, patience, and encouragement throughout the process of finalizing the thesis.

I would also like to thank Dr. Diana Yu of the Gage Lab for her advises and assistance with the cell culture aspects of the experiments, including provision of the rat hippocampal progenitor cells and culturing them along with nanowire chips for the study.

Also, I would like to thank all members of the Wang Lab for their support and assistance, especially Ke Sun, for providing samples of SiNW chips for the study and for his assistance with the SEM imaging of the wires as well as assistance in putting together text for nanowire synthesis process portion of this thesis and related figure images.

Finally, I would like to thank Jennifer Meerloo at the UCSD Neuroscience Microscopy Facility for her assistance with confocal microscopy images of the cell-nanowire mixture with Olympus FV1000 confocal microscope. Neuroscience

equipment maintenance is funded by the UCSD Neuroscience Microscopy shared Facility Grant P30 NS047101.

ABSTRACT OF THE THESIS

Silicon Nanowire Compatibility Analysis with Rat Hippocampal Progenitor Cells for use in Neuroprosthetics Development

by

Eun Kyung Joanne Lee

Master of Science in Biology

University of California, San Diego, 2014

Professor Deli Wang, Chair
Professor Willie Claiborne Brown, Co-Chair

Nanomedicine is one of the most promising areas of nanotechnology, aspiring to use nanoparticles and structures to diagnose, analyze, and treat medical conditions. Current research in nanomedicine relies on larger scale measurement and there has not

been a study that shows how the individual cells react to the presence of nanoparticles. It is our belief that understanding how a cell reacts and interacts with semi-conducting or metal nanostructures, specifically nanowires (NW) is important for designing future nanodevices, particularly Neuroprosthetics.

Adult rat hippocampal progenitor cells from female Fischer 344 rats were cultured to be kept in its undifferentiated state and were allowed to settle by gravity on top of three types of NW chips – ones with horizontal, vertical, and random growth of silicon nanowires to answer the following questions: 1. Are cells viable with nanowire structures? 2. How does the cell interact with nanowires by observing changes in cellular component, specifically cytoskeletal movement (contents or arrangements) when in contact with the NWs. Results showed that there were significantly less viable cells found on horizontal NWs than vertical ones, although mechanical difficulty with imaging vertical NW may have contributed to death or loss of cell interaction with NW on imaging. There was evidence of cells actively and preferentially interacting with NWs with horizontal NW chips. Future direction of the study would be to use NWs to stimulate and detect electrical activities within the cell and study how the ion gradients are affected in/around the cell.

Introduction:

What *is* Nanotechnology? Nanotechnology is a manipulation of materials at nano-scale to create specific chemical and physical properties and functions at a molecular or an atomic level (1). A nanometer is one billionth of a meter –for comparision, consider other familiar elements: DNA is about 2.5 nm long, and a sodium ion is about 0.2 nm in diameter. The miniscule dimensions of nano-devices are stirring up much excitement in the scientific community because it allows for unique interaction with cells and organisms at subcellular and/or molecular level.

Another interesting fact of nano-particles is that they exhibit different physical properties at nanoscale than what is well known to be their property at macroscale. For instance, gold particles are solid at room temperature in macroscale, but are liquid in nanoscale; silicon is normally an excellent insulator but becomes a conductor in nanoscale; opaque materials such as copper turn transparent at nanoscale.

Technological advancement has brought nanotechnology into many aspects of our lives, from nano-coated textiles to cancer therapy. Of the many fields of research for nanotechnology, Nanomedicine is one of the most sought after field, with much hope and aspirations to use the unique properties of nanoparticles for the purpose of diagnosis, analysis, and treatment of physical ailments. In this experiment, we attempted to lay the ground work for developing a neural prosthesis operating at nanometer scale by interfacing rat hippocampal neurons with functional

semiconductor nanowire (NW) devices and studying its apparent relationship via imaging methods.

Of various types of nanomaterials available, nanowires were chosen for its unique conductive property to be able to stimulate and/or detect electrical stimulus. With proper grid system to guide processing of the information obtained from a nanowire chip, one can increase the sensitivity of detecting changes in electrical currents within a system – even that of a single cell, depending on the size of the wires. Naturally, neurons would be the cellular system of choice for analysis with an electrically sensitive device such as nanowires.

Neurons' normal function involves constant communication through electrical stimulus and responses to both intracellular and extracellular processes. Once damaged, however, neurons of Central Nervous System (CNS), unlike the neurons of the Peripheral Nervous System (PNS), were found not to regenerate and reinstate its original connection and communication. Over the years, it has been found that the neurons of CNS do attempt to regenerate but its attempts are overpowered by the vast range of inhibitory signals (2-10). Various studies have been done to identify the origins and mechanisms of these inhibitory signals to counteract neuron's regenerative efforts, and now grafting various cell types – from fetal CNS neurons, peripheral neurons, specific lines of astrocytes (C6-R cells), macrophages, and Schwann cells – unto the damaged adult CNS have shown varied success in rescuing damaged neurons to stimulating regeneration and recovering function (11-17).

Therefore a system of microelectrode system consisted of biocompatible nanowires may provide insight into the activities of normal and damaged neurons in the brain and in the peripheries, to assist in finding ways to stimulate regeneration or reconstitute damaged CNS (whether due to neurodegenerative diseases or trauma) through neuroprosthetics development. However, neurons are not the only cell types that communicate via electrical stimulus. All cells in the body are filled with and surrounded by ionic charges – whether it is charged proteins or ionic molecules. Ionic gradients and resulting currents are an essential part of cell communication and are influential in many cellular processes. For example, determining whether the hyphal tip will grow in fungi (24), or inhibiting or promoting communication between neighboring thyroid follicular cells (26) are all based on ionic gradients and resulting currents in an intracellular and extracellular environment. Hence, nanowire based microelectrode system may be used to study all types of cells and processes.

Even for nanoscale drug delivery system developed to overcome drug resistance in cancer chemotherapy (27) nanowire array may provide an advantage over currently available protocol for testing effectiveness of the chemotherapy. Currently, drug resistance is said to be prevalent if there are no size reduction observed for the tumor in treatment or a relapse occurs after a ‘successful’ completion of a treatment program (28). Many mechanisms have been proposed to compensate for the multi-drug resistance genes. For example, increase in intracellular and vicinity concentration of drug at the target cancer cells were accomplished by up-regulating the rate of endocytosis and by modifying the biodistribution of the drug using an improved

mechanisms for specific targeting, respectively(28).

Frequently, molecular analytic techniques for studying certain gene or protein expression from cell lysate or a crude estimation of size reduction of a tumor is used to determine effectiveness of an antitumor drug. Obtaining data of the changes in a single cell level for the purpose of observing drug effects over time is difficult to record due to the physical limitations of currently available probes and electrodes. The small size and versatility of biocompatible nanowire array can overcome such barriers to be used as a nanoprobe to detect and stimulate at a single cell level.

Introduction on Nanowire variety

For the experiments, Silicon nanowires were chosen for its known biocompatibility and simplicity for production.

There exist many different methods for NW production, including Top-down etched Silicon nanowires and bottom-up self-assembled semiconducting nanowires. The NWs can be arranged both vertically and horizontally. Each type and arrangement of wires has their own advantages and disadvantages:

Vertical nanowires are made either through a top-down or a bottom-up approach. A top-down approach indicates a starting material is etched or broken down to form the grooves around the wires and a bottom-up approach indicates a catalyst is used to initiate self-assembly to form growing strands of wires; for example, in our experiments, Silicon nanowires are etched out through a top-down approach from a p-Silicon wafer block using metal assisted chemical reaction, while semiconducting wires are built through self-assembly starting from a catalyst seed.

In general, vertical wires are formed in a relatively uniform, predictable pattern depending on the initial placement of catalysts for semiconducting or metal wires or by the etching protocol used. However, due to physical limitations of the components used for seeding, there are limitations in wire density achievable for a given area. Also, while seeded semiconductor wires may form too dense of a wire forest, random-array semiconductor wires tend to form too sporadically around an area, making semiconductor wires more difficult to work with. Vertical Silicon wires on the other hand have a very uniform organization as etching is done by metal-assisted chemical reaction. The wire density depends on the reaction between the substrate and the etching solution and for that reason it is difficult to create varied versions of the chips in terms of its wire density. The technique we used to make vertical Silicon nanowires is a widely used, cost-effective technique for large scale synthesis of Si nanowires arrays at low temperature (Figure 2). This technique was initially proposed by a group from China (4). Authors suggested a growth mechanism in the initial paper and then published the detailed descriptions regarding the chemical etching process in a later paper (5).

Length of the vertical wires were controlled by the duration of the etching or self-assembly time, while the diameter of individual wires were not. However, the main difficulty we had with the vertical wires in the study was the lack of a reliable, convenient method to invert the cell-NW mixture to make it compatible to image with an inverted microscope. The opacity of the substrate base along with its dense wire

forest on top, light could not penetrate from the bottom and image the wires and the cells on top surface of the chip.

Horizontal nanowires are made by sheering off the vertical nanowires from their base via ultrasonication and suspending them in a volatile solution such as isopropanol before spraying it onto a surface to dry, allowing the wires to adhere to the surface while the volatile liquid vaporizes. Horizontal wire suspension system provided a versatile platform to try different density of wires as well as various surface materials and was convenient for transport of materials and simplified chip preparation. Also, by using thin and transparent material as the substrate, we were able to use an inverted microscope to image the chip-cell culture mix without harming the wires or the cellular networks. However, it was common to have an uneven spread of nanowires throughout a given surface area, resulting in clumps of wires found in some areas while no wires were seen in other areas.

Materials and Methods

Nanowire Substrates:

Vertical Silicon Nanowires from metal assisted etching (vertical SiNW): P-type Boron doped Silicon wafers at 1-0-0 orientation (1-5 Ω cm^{-1}, waferworld) were cleaned with solvent, rinsed with DI water and dried with N_2. The metal-assisted chemical etching process was applied to the cleaned Silicon wafers in aqueous solutions of 0.02 M Silver Nitrate ($AgNO_3$) and 5 M Hydrofluoric acid (HF) with gentle stirring. The solution was kept at a constant temperature of 50°C. Their model and equations describing the etching process are shown in Figure 1, and the home made etching setup is shown in Figure 2. After etching, wafers were gently spray rinsed with DI water and then silver coating formed on the nanowires were etched in nitric acid. Samples were then spray rinsed with DI water again and dried with N_2 (3,6). 2" wafers were then cut to 2 x 2 cm^2 pieces for investigation. For chips that were to be treated with critical point drying before being imaged using SEM were cut into bigger pieces (7.5 x 7.5 cm^2).

Horizontal Silicon Nanowires (horizontal SiNW): A horizontal etched SiNW chip was made following the same procedures as for vertical SiNW chip and then was ultrasonicated (50W for 2 minutes in isopropanol) to dissociate individual nanowires from the base of the chip. Some of the samples were exposed to centrifuge to remove bigger bundles of nanowires. This method allowed us to prevent leaving large bundles of nanowires behind on the silicon substrate. Figure 4 shows the substrate after ultrasonication—it is clear to see patches of nanowires missing from the array. Once

dissociated, horizontal nanowires were sprayed onto a substrate surface to dry and allowed to adhere to the surface while the volatile liquid vaporizes.

Concentrated SiNW solution was made by transferring isopropanol solution with loose nanowires separated through ultrasonication process, into a spray bottle. Before each experiment, the mixture was sprayed uniformly as possible, onto a glass slide surface and then left to dry for 5-10 minutes. During spray, the distance and interval spray time were kept constant, while the substrate (glass slide) was rotated for an even coating all throughout. Figure 5 shows the concentrated SiNW suspended in isoproanol and SEM images of the horizontal SiNW sprayed onto a glass slide.

Nanowire synthesis

The nanowires length is dependent on the etching time while the diameter of the nanowires does not show significant change. Figure 3 shows the effect of increased etching time (5, 10, and 20 minutes) on the length of the nanowires on p-silicon wafer– longer the etching time, the longer the nanowires are. For Figure 3a, 5 minutes of etching time resulted in average NW length of 580nm; Figure 3b, 10 minutes of etching time resulted in average NW length of 1.5μm; and Figure 3c, 15 minutes of etching time resulted in average NW length of 2.8μm. Average diameter of the nanowires does not fluctuate very much regardless of the length of the etching time; the average diameter was found to be in the range of 36 to 260nm for all three etching times. The images were taken after cleansing with diluted nitric acid. Figure 3 shows both the optical image of the etched nanowires arrays on a full 2” wafer as well as the side view of the nanowires structures were characterized using ultrahigh resolution

scanning electron microscopy (HRSEM: FEI XL 30 with FEI Sirion column). Edges and the backside of the 2" Silicon wafer were protected from the etching solution. In the image of the wafers after etching, the area with nanowires show up as a darker region compared to the surrounding area without etched nanowires due to the light absorption in the SiNW array; therefore with the longer etching time, the intensity of the dark region is shown to increase.

The nanowires shows smooth surface, well-vertically aligned, and shows uniform diameter along the length of the wire. The etching process shown has an average etching rate of 110 Å/s. EDAX study shows no evidence of Ag particles left over in the silicon nanowires arrays.

Cells and Reagents

Adult rat hippocampal progenitor cells (HCN), a type of stem cell was chosen for its hardy, easy growth requirements and for its versatility to differentiate into various neuronal cell lines. These cells are generally around 10-15 microns in diameter in their undifferentiated state, which is characterized by a round cell shape with few tiny processes radiating from the body.

The adult neuronal progenitor cells were isolated and passaged originally from hippocampi of adult (>3 months) female Fischer 344 rats in accordance with procedures approved by the University of California San Diego and by the National Institute of Health (2). Cells were suspended in serum-free medium: Dulbecco's modified Eagle Medium (DMEM)/F12 (1:1) high glucose medium (Irvine Scientific) with N2 supplement (GIBCO) and 20 ng of recombinant human FGF-2 per ml (R&D).

Cultures were incubated for up to 6 days and with medium change every 2-3 days with fresh medium containing FGF-2. Plating density was approximately 10,000 cells/cm^2. All buffers and media were made immediately before use. The cells were maintained following standard sterile procedures.

NW chips were sterilized in UV light for 30 minutes before plating cells on top. Cells were washed with PBS (Invitrogen), dissociated from the culture plates using TrypLE™ Express (Invitrogen), then was washed with PBS again, and then suspended back in cell culture media as described earlier. The diluted volume of cells is then plated on top of the sterilized NW chip. Cells were left to settle on top of the NW chips by gravity.

If the cell-chip mixture were to be imaged immediately after plating, as soon as the diluted volume of cells were plated on top of the sterilized NW chip, it was taken over to the imaging center, and was imaged approximately 20-30 minutes after plating. Otherwise, the cell-chip mixture were then incubated for an additional length of time and when it was ready to be imaged, the cell-chip mix was taken out of the culture media and was suspended in Dulbecco's Phosphate-Buffered Saline (DPBS) without Magnesium and Calcium (Invitrogen) before taken over to the imaging center.

Imaging

Live/Dead cell assay using Calcein-AM and Ethidium-Bromide:

Calcein AM and Ethidium homodimer (EthD-1) was added to all cell-wire mixtures that are imaged. *The Live/Dead© Viability/Cytotoxicity Kit* (molecular probes) reagent solution was used following manufacturer guidelines and protocols.

Calcein AM is a cell-permeable dye that is used as a live cell indicator. It requires an intracellular esterase ubiquitous to a healthy living cell to undergo an enzymatic conversion from the nonfluorescent state to the fluorescent state. Fluorescent Calcein AM emits strong green fluorescence at excitation/emission wavelength of ~495 nm and ~515 nm, respectively (molecular probes).

Ethidium homodimer-1 (EthD-1) is a dead-cell indicator dye that selects for cells with lost integrity of plasma membrane, such as cytotoxic or apoptotic cells with damaged membranes. In a damaged cell, the nuclear envelope dissembles and releases broken pieces of DNA into the cytoplasm. Therefore, once inside the cell, EthD-1 is able to bind to nucleic acids and undergo 40 fold enhancement of its fluorescence to produce intense red fluorescence at excitation/emission wavelength of ~528 nm and ~617 nm, respectively (molecular probes).

Laser Scanning Confocal Microscope:

Olympus FV1000 laser scanning confocal microscope was used to image horizontal SiNW and fluorescently labeled cells using Live/Dead© assay kit. The isopropyl suspension of horizontal SiNW was sprayed on top of slides and air dried before a drop of labeled cell culture suspension was placed on top. The slide was then incubated at 37 deg. C for 10 minutes for cells to settle by gravity. Slides were imaged using both confocal microscopy and DIC setting to identify and confirm locations of individual or bundles of SiNW as they are not auto-fluorescent for easy visualization. For cells emitting either green or red fluorescence, its shape is outlined by the fluorescence, so few single or bundles of wires that are directly associated with the

cell are seen by blockage of the cellular fluorescence. Control images of live/dead cell assay and DIC correspondent image is shown in Figures 6 and 7.

Scanning Electron Microscopy

Before imaging, the cell-chip mix was fixed in 5% Formaldehyde and rinsed with PBS. To completely dehydrate the sample before imaging it using Scanning Electron Microscope (SEM), the SiNW chip sample was dehydrated in 99% ethanol and critical point dried (Tousimis 815A CPD). When the chamber pressure stabilizes around 1350 psi (+/- 5% of 20 deg C) and the temperature achieves 31 deg. C, the critical point is considered achieved and undergoes tousimis equilibrium cycle. Tousimis equilibrium is the point during the critical point in which both the pressure and temperature are maintained above the critical point within the chamber for a period before the chamber is decompressed. Once the sample is dried, it was sputtered (~10nm thick layer) with Chromium using Emitech K575X. the sample was then studied in a scanning electron microscope (HRSEM: FEI XL 30 with FEI Sirion column).

Results and Discussion

Calcein AM and Ethidium homodimer-1 (EthD-1) was used as live/dead cell assay (Figure 6) but also to visualize cells under fluorescent imaging systems, including laser scanning confocal microscope (Olympus FV1000). The nanowires itself are not coated with fluorescence and are not visible under florescence microscopy. However, by visualizing the entire intracellular space of both dead and live cells using red and green fluorescence of EthD-1and Calcein AM, respectively, we hoped to locate nanowire presence by locating the blockage of cellular fluorescence by nanowires. DIC settings were also used to confirm the location of nanowires seen in the fluorescent imaging as well as to complement the data by revealing the presence of other NWs present nearby.

Fluorescent microscope

Initially, cells were cultured on top of two types of NWs, Vertical etched SiNW and sprayed horizontal SiNW for two days then fluorescent images of cells with Calcein dye was taken using a bottom-light source microscope. Images were taken at 10x, 20x, and some at 40x amplification, and found that in general there were very little live cells on the chips. Mainly small pecks of green fluorescence (assumed to be cellular components) along with a few clusters of live cells were found on vertical NWchips. On the other hand, larger clusters of live cells on a visibly marked bed of horizontal SiNW were seen on the horizontal chips (Figure 8). During this imaging session, we first noted, there was areas in vertical SiNW chips with a patterned surface not unlike a cell groove, but was too uniform to be believed as a cell groove. No such

pattern was noted on horizontal array SiNW chips. These same chips were taken to be imaged using scanning electron microscope (SEM) a week after the cells were fixed onto the chips using formaldehyde.

Scanning Electron Microscope (SEM)

A thin coat of metal was put on top of the fixed cell + chip sample to enhance the visual image of cellular/biological components, if any, prior to imaging with the SEM. Imaging revealed all of the vertical wires that were damaged and broke with few spikes of wires that were covered with a sticky looking unknown material. No cells seemed to be present at the time of EM.

It was not surprising there were no cells at the time of imaging as it had been a week since the cells were fixed onto the chip and then kept in PBS. However, it was still a good opportunity to take a closer look at the patterned surface seen during the fluorescent microscopy.

On the Vertical NW sample, round, regularly shaped imprints were found on SEM, corresponding with the uniformly patterned surface seen with fluorescent microscope (Figure 10). Comparing with the initial imaging of the vertical SiNW chip during production, these 'patterned' grooves were definitely a new occurrence. On closer zoom, edges of these grooves seemed to be more geometric; making it less likely it was due to direct cellular presence on top of the wires. (Figure 11)

On the other hand, on horizontal NW sample, there was surface finding that seemed to correlate with the cell cluster finding in earlier fluorescent imaging (Figure

10). There were areas of the chip that looked like it was crushed by something on top, and pushed aside to form something like a nest (Figure 11). The direct surface of such areas on zoom seemed to have eroded with sticky coverings on top of the wires (Figure 11). The sticky overlay on top of the wires may be extracellular matrix protein deposited by cells having lived there. Anchorage-dependent cell, such as neural cells, secretes matrix proteins including, but not limited to, collagin, elastin, laminin, etc., to help them hold onto the surface via integrins that are attached to intracellular cytoskeleton.

Olympus FV1000 Confocal Microscopy

For the confocal microscopy, we had control image taken with cells alone on coverslip to show clear live/dead cells through fluorescence (Figure 9) and confirm with DIC (Figure 10). For the experiment, we had the horizontal SiNW sprayed, dried, and then the cell mixture were put on top of glass slides. No vertical NWs were used at this time due to the limitations in inverting the chip for imaging (bottom light source) without disrupting cellular/wire interaction and environment.

Although we hoped the cellular fluorescence would be enough to indicate when there is a NW penetration into the cellular membrane, only bundles of wires were able to successfully block enough fluorescence of a cell to clearly indicate its location in the confocal images, confirmed by DIC image comparison. The confocal images showed clear embedding of the horizontal nanowire pieces on the outer surfaces of the cell.

In all of the samples, there were no indications of NW penetration induced apoptosis, as no correlation was noted between the extents of nanowire interface with the cellular membrane with the rate of apoptosis.

What was probably more interesting to note was the seemingly high affinity adherence of cells to bundles of nanowires, characterized by a flat border of the cell on the side attached to the nanowire bundles and rounded boarders of rest of the cell on the glass slide (Figure 9). Considering the fact that the wires were first sprayed on the substrate, dried, and then a drop of cell culture mix (cells, media, dyes) were put on top, it was surprising to find preferential clustering of cells around where there were higher concentration of nanowires. In some cases, the cells seemed to even have 'squeezed' itself into a branch formed by two separate nanowire bundles to obtain two flat surfaces and a rounded top to resemble the shape of an ice cream cone (Figure 10). This phenomenon was found all throughout the slide and the cells seemed to prefer adhesion to wire bundles, resulting in formation of a cluster of cells around set of bundles of wires, and relatively empty space around the cell/wire complexes. These results may be due to some form of structural connections being formed between cellular matrix and the NWs that makes it preferable for cells to adhere to than the glass slide. Or, there may also be some kind of electrical field that might be changing ion concentrations around the NWs that works to attract the cells towards the NWs, but it may be just a theory at this time. We considered making the NW fluorescent and visible by adding fluorescent particle coating such as using Quantum Dots or conjugated fluorescent proteins, but as it may alter the surface chemistry that may as

well be the cause of the unique findings in the experiments, we decided to continue with comparison imaging with DIC to confirm locations of NW complexes instead. GaAs NWs have red fluorescent emission naturally, but is considered more toxic to cells to be used in this experiment.

Next, SEM imaging of vertical SiNW cultured for 30 mins vs. 2 days with and without cells was done. The samples without any cells were to be used as control to see if the cellular culture media was the culprit of NW dissolution. The result showed the wires without cells at 30 minutes without any degeneration, but at 2 days it showed much degeneration and was covered by the same sticky, unknown material (Figure 14). Meanwhile the sample with cells showed many cell-like structures at both 30 minute and 2 days of culture. In the cellular sample, a higher concentration of sticky surface covering was found around the cells (Figure 15A). As if the surface covering were solely due to ion or protein deposition from the media, there should be an even spread of the materials throughout the chip regardless of where the cells were found, however the imaging showed concentration of the material on and around the cells only. A close up of the edge of the image shows that there's a clear border between regions of wires that are being 'invaded' by the sticky materials and the regions that are free from it (Figure 15B).

A longer culture of the cells lasting 18 hours and 6 days were done. With 18 hour culture time, wires were still healthy and cells were seen (Figure 16). However, at 6 days duration, there was severe NW degeneration with no cell presence (Figure 17). This time, a technique called the Critical Point Drying (CPD) was used to

preserve the cellular environment prior to SEM and it showed a much more vibrant, but fragile, cellular structures. There was a differentiated neuron-like cell with processes that seemed to be reaching out to another bed of NWs at 18 hour culture time (Figure 16).

Overall, it was confirmed that as culture period lengthened the SiNW structures further degenerated and the cell viability seemed to go down accordingly (Figure 17, 18).

Next step in the research would be to observe how the cell interacts with NWs by observing changes in cellular component, specifically cytoskeletal movement in terms of its contents or arrangements when in contact with NWs. It would be also very interesting if a serial time-lapse imaging can be done to see whether cells seek out nanostructures and whether they actively rearrange its cytoskeletal components to engulf and/or form focal adhesions with the nanostructures. Ultimately, NW can be used to stimulate and detect electrical activities within the cell. If detection of electrical potential using nanowires are comparable to current methods to measure intracellular/extracellular charges and electricity (such as using small electrodes and glass pipettes used in patch clamping), then NW electrode may be beneficial to be developed for use.

Conclusion

In conclusion, though Silicon may not be intrinsically cytotoxic to cells, it seems with exposure to devices such as SiNW chips over an extended period of time may result in internalization and accumulation of Silicon particles in excess, resulting in loss in cell viability and ultimately result in cell death. A separate study done in Germany showed that SiO2 nano-scaled particles (as are several other nano-sized particles) are internalized by human endothelial cells and that an impairment of the proliferative activity and a pro-inflammatory stimulation were induced by SiO2 particles (29), providing possible support for the conclusion.

Biodegradability of Silicon may be a valuable asset for making devices such as a silicon drug release system. By taking advantage of the natural degradable property of Silicon, a multiple-layer Silicon capsule may be developed to encase drugs for slow release over time; by limiting extracellular space exposure to the outer most surface and allowing degradation, drug encapsulated in the space between the layers of silicon may be released and expose the next layer of silicon for further degradation. However, the low cell viability correlated with long term exposure to SiNWs as shown in this study poses new questions for current studies done with other nanostructures made purely with Silicon nanoparticles. If they saw reduction in tumor size using drug delivery system using Silicon nanostructure, the true source of death of tumor cells should be confirmed to show whether the effect is due solely based on drug effectiveness or if it may be due to toxicity of degraded silicon uptake and accumulation by the cancerous cell. Nonetheless, further study is needed to determine

the rate of degradation of Silicon from a nanostructure, whether it be a nanochip or a capsule, and also the rate of intracellular absorption and accumulation of the degraded Si particles and its level of cytotoxicity before further uses (especially long-term) of nanowires can be determined.

Figures

Figure 1: Metal assisted Si etching mechanism

$$4Ag^{+}(aq) + Si^{0}(s) + 6F^{-}(aq) \rightarrow 4Ag(s) + SiF_6^{2-}(aq)$$

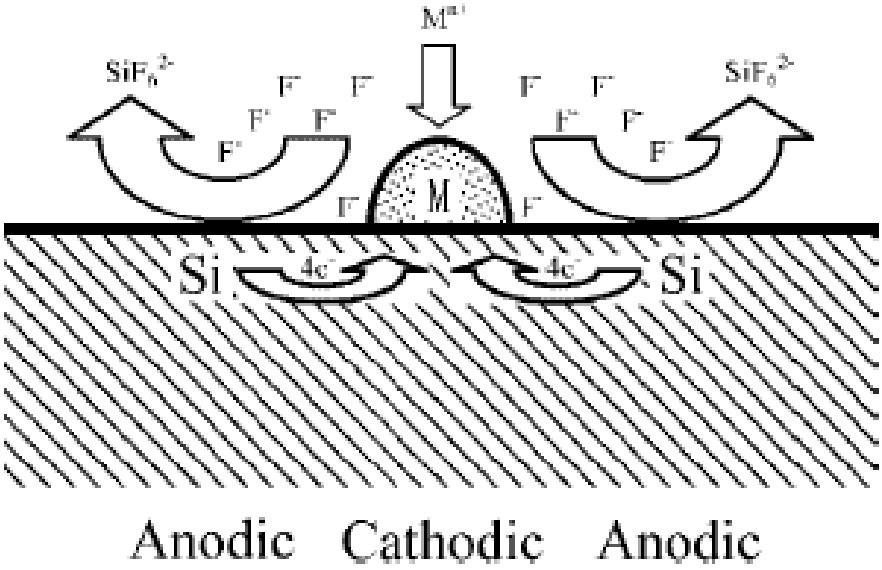

Figure 1: P-type boron doped Silicon (100) wafers (1-5 Ω cm^{-1}, waferworld) were cleaned with solvent, rinsed with DI water and dried with N_2. The metal-assisted chemical etching process was applied to the cleaned Silicon wafers in aqueous solutions of 0.02 M AgNO3 and 5M HF with gentle stirring. The solution was kept at a constant temperature of 50°C. After etching, wafers were spray rinsed with DI water and then silver coating formed on the nanowires were etched in nitric acid.

Figure 2: Si etching setup

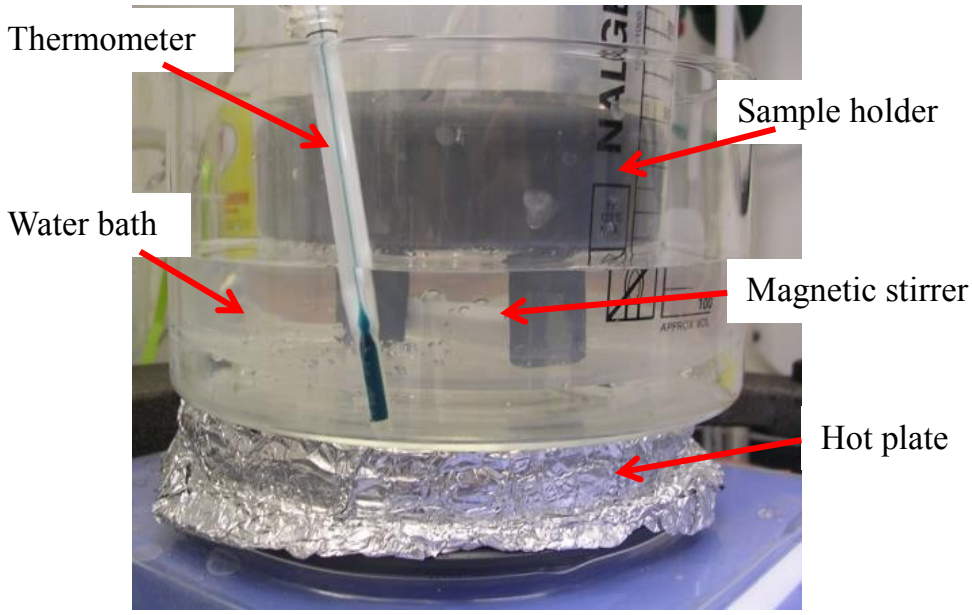

Figure 2: Homemade Si etching set up contains a thermometer, a hot plate, a magnetic stirrer to keep the reaction at a constant temperature of 50°C in the water bath and a sample holder to hold the Si wafer.

Figure 3: Si etched for different amount of time: a) 5 min, b) 10 min, c) 20 min

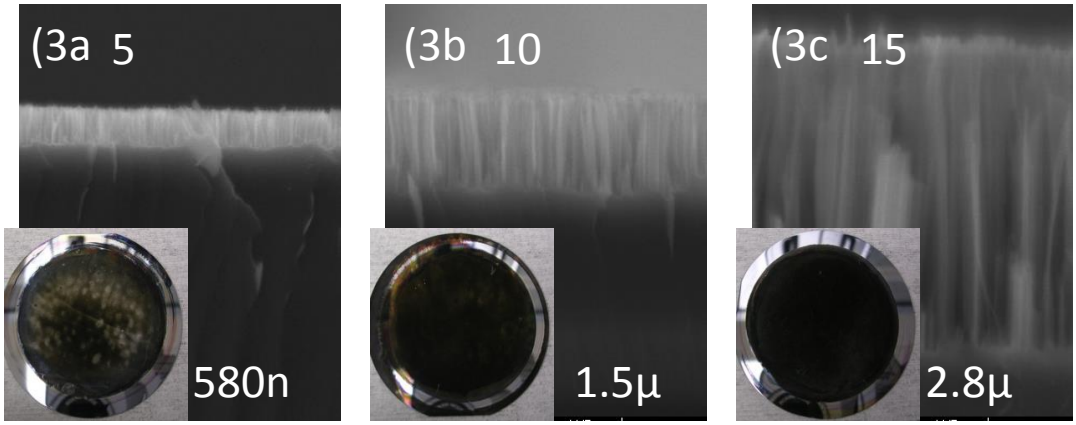

Figure 3: the effect of increased etching time (5, 10, and 20 minutes) on the length of the nanowires on p-silicon wafer. Fig 3a, 5 minutes of etching time resulted in average NW length of 580nm; Fig 3b, 10 minutes of etching time resulted in average NW length of 1.5µm; and Fig 3c, 15 minutes of etching time resulted in average NW length of 2.8µm. The average diameter was found to be in the range of 36 to 260nm for all three etching times.

Figure 4: Si substrate after ultrasonication in different magnification levels

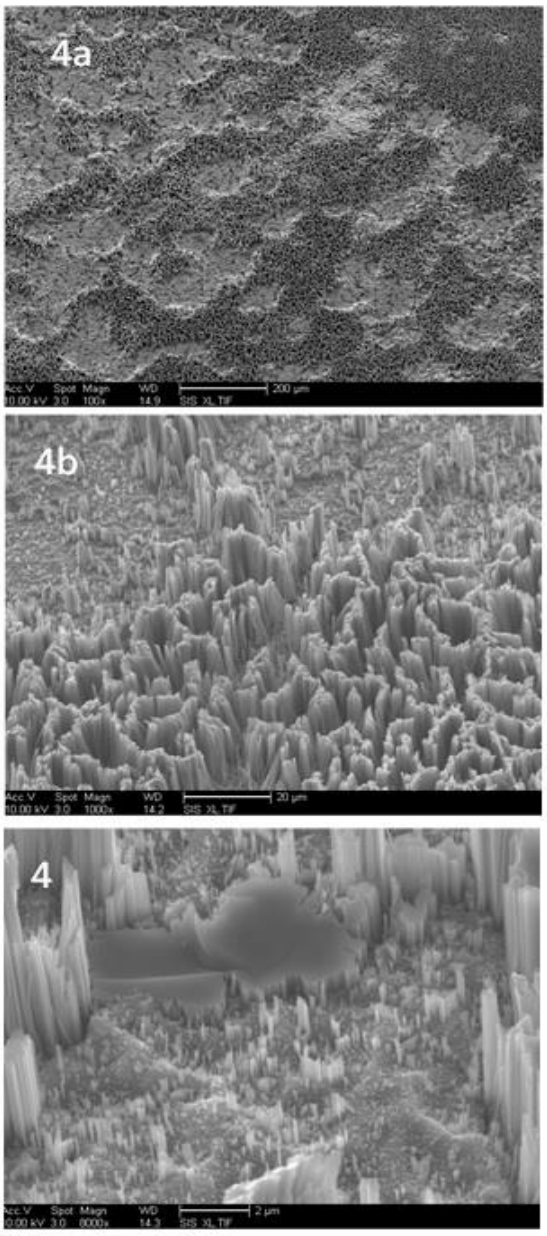

Figure 4: Silicon Wafer substrate after ultrasonication. A) 200 micron, B) 20 micron, C) 2 micron magnification

Figure 5: Horizontal SiNW preparation and SEM images

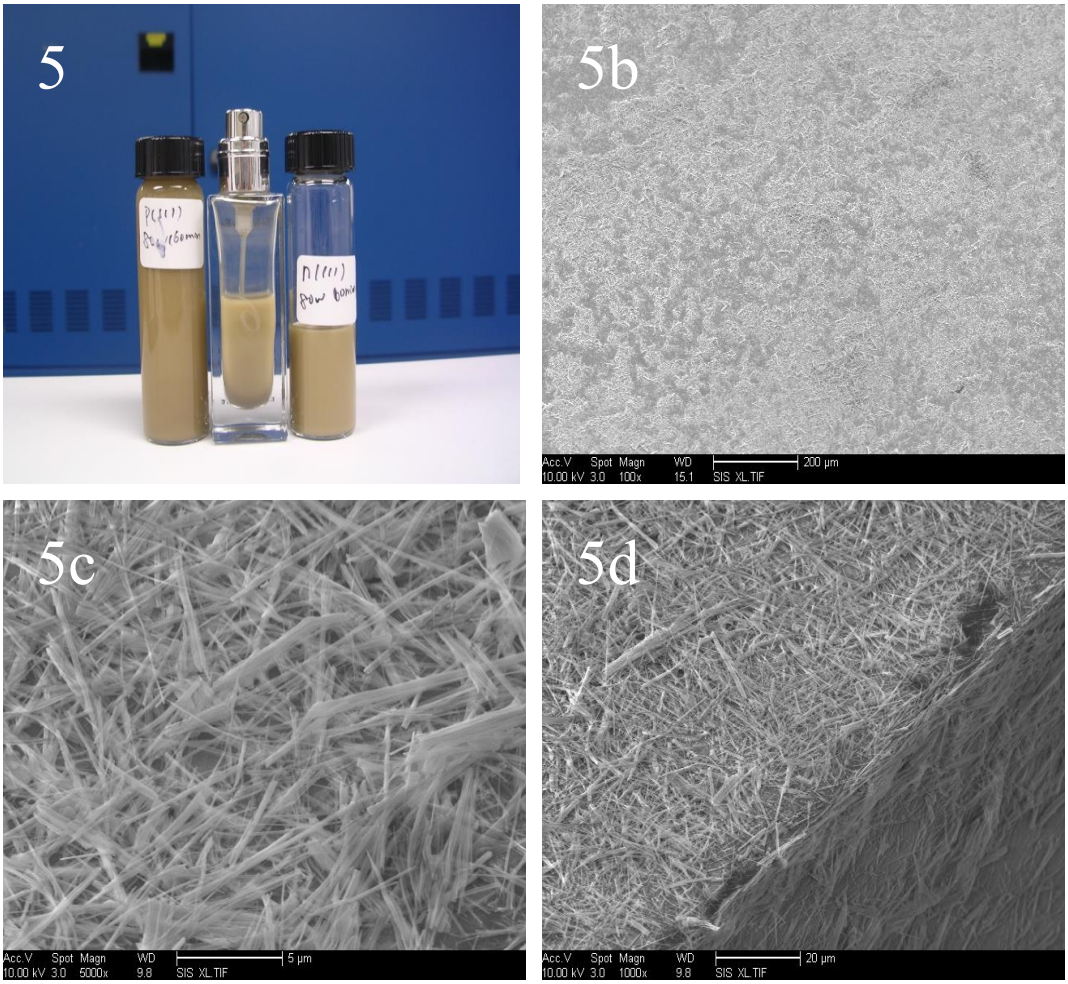

Figure 5 a) concentrated Silicon nanowire (SiNW) suspended in isopropanol solution, (b-d: SEM images of the horizontal SiNW sprayed onto a glass slide) b) large view of sprayed glass substrate showing a fairly uniform coating, c) non-uniform silicon nanowires on substrate, and d) coating at the edge of substrate.

Figure 6: Live/Dead cell assay using Calcein-AM and Ethidium-Bromide

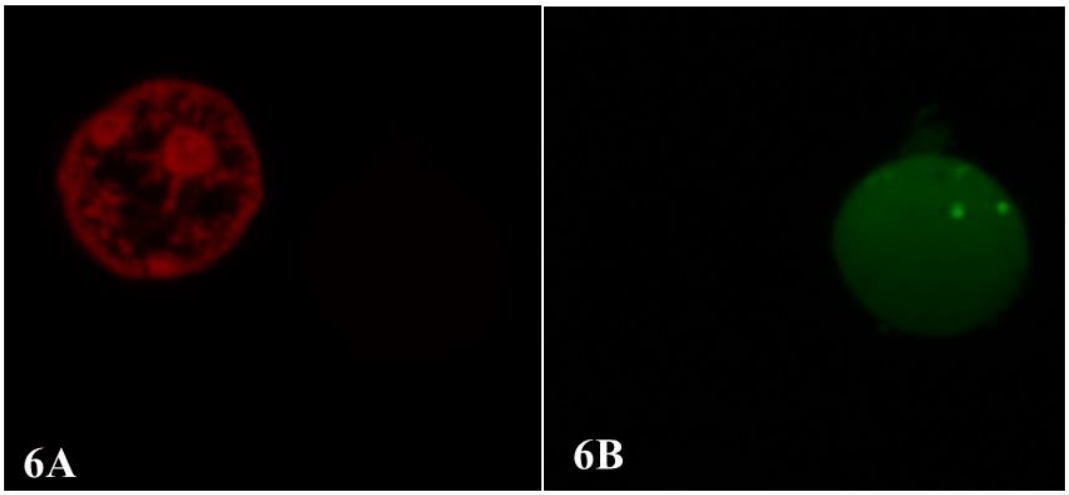

Figure 6 a) Dead cell staining using Ethidium Bromide dye (fluoresce Red-Orange): one of the simplest methods of determining cell death due to the property of EtBr to bind to DNA strands. In dead cells, the nuclear envelope dissembles and releases broken pieces of DNA into the cytoplasm. EtBr enters the cell through a leaky plasma membrane and binds to these DNA bits. **b)** Live cell staining using Calcein AM (fluoresce Green): requires intracellular esterase that is only present in live cells to cleave off an acetomethoxy group and to expose its active site to chelate calcium ions. Once it binds to calcium, it strongly fluoresces in green and it is trapped inside the cell.

Figure 7: Live/Dead cell assay confirmed with DIC imaging

Figure 7: DIC (differential interference contrast) imaging is contrast imaging done by converting phase changes detected as light traveling through areas with different light refractive indexes into amplitude changes. It is mainly useful for achieving an overall image of a live cell/living tissue without having to fix it. This image shows the previous two cells shown in Figure 6 (live cell on the right, dead cell on the left) present right next to each other. Both cells were in the control slide, with no presence of NW's. Using DIC we cannot tell which ones are dead or alive with certainty. Cell shown is approximately 15 um.

Figure 8: Fluorescent images of cells with Calcein dye after 2 days of culture on horizontal vs. vertical SiNW chip

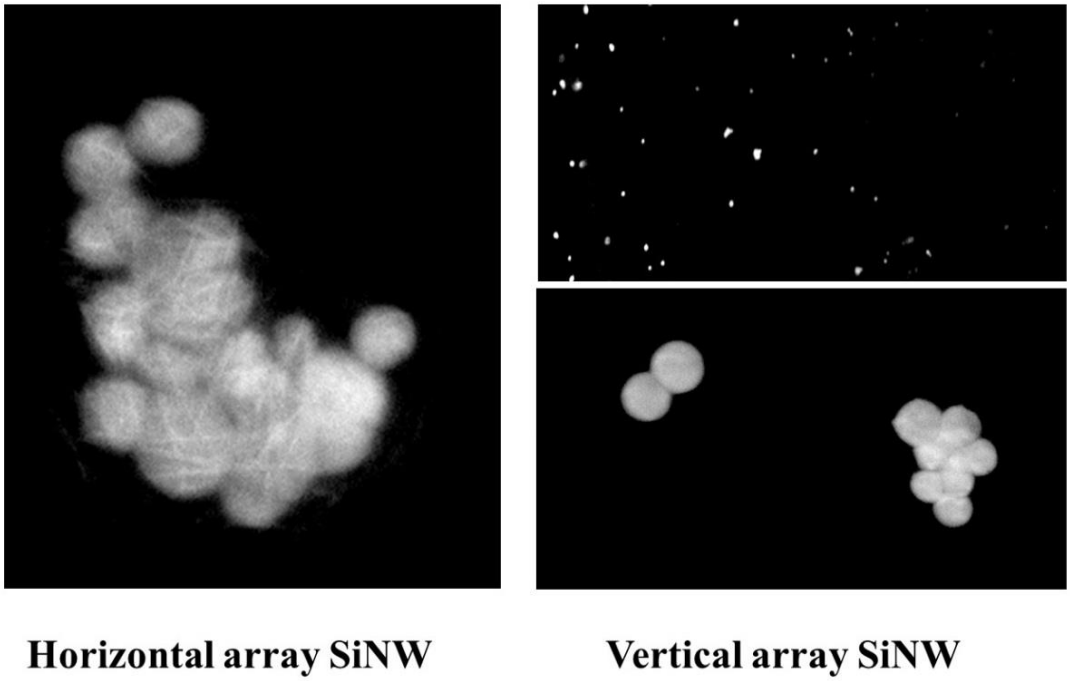

Figure 8: Pecks of green fluorescence (cellular parts) on vertical NWchips and few clusters of live cells vs. larger clusters of live cells on a bed of horizontal NW chips. Cells were fixed with formaldehyde onto the chips after 2 days of culture and were kept on PBS solution until imaging.

Figure 9: Vertical array SiNW imprint

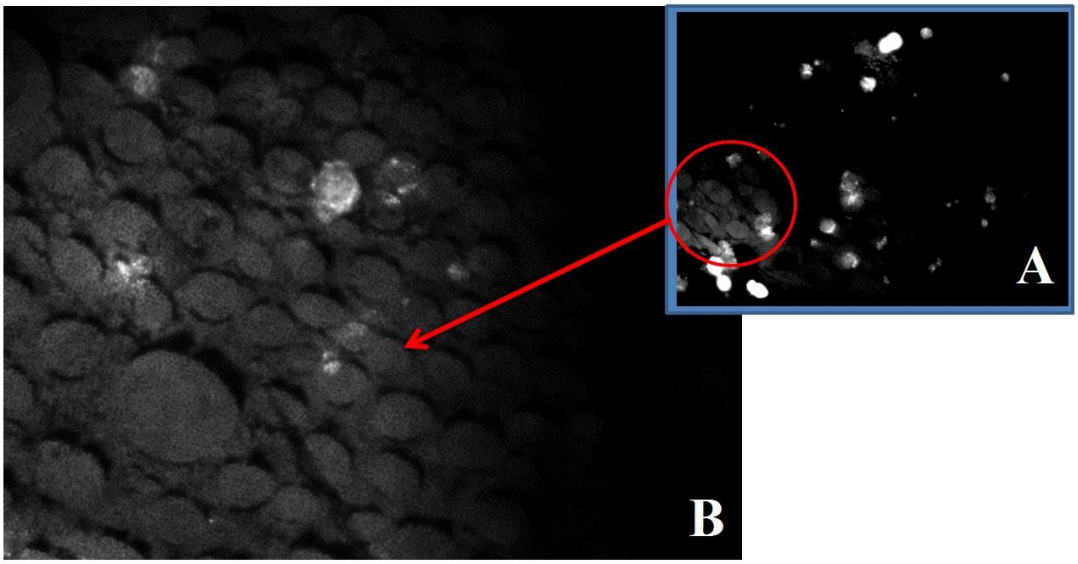

Figure 9: First noted during initial fluorescent imaging, it looked like a patterned surface not unlike a cell groove, but was too uniform to be believed as a cell groove. No such pattern was noted on horizontal array SiNW chips.

Figure 10: comparison of chip surface fluorescent imaging vs. SEM

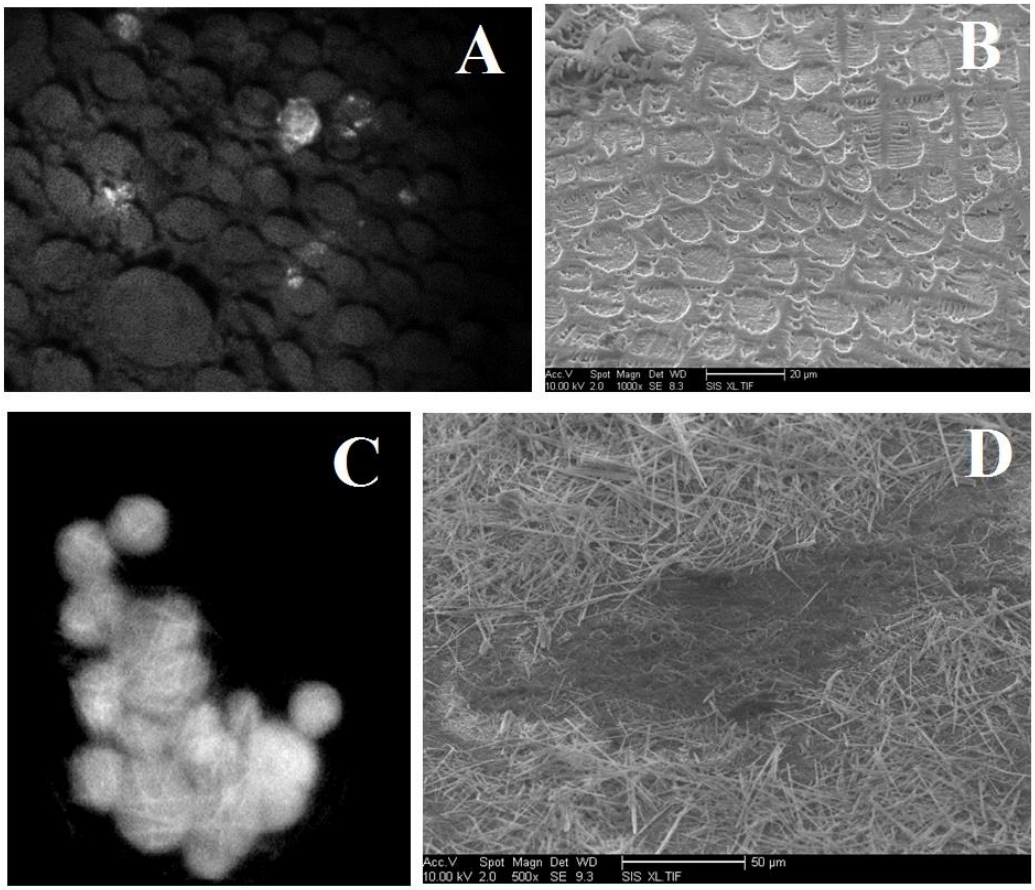

Figure 10: corresponding surface imaging. A) patterned surface of vertical SiNW on fluorescence imaging, B) corresponding patterned surface of vertical SiNW on SEM. C) Cellular cluster with visible horizontal (sprayed) NW shadow, with D) evident cell groove on surface of horizontal NW chip on SEM.

Figure 11: comparison of chip surfaces for vertical vs. horizontal SiNW

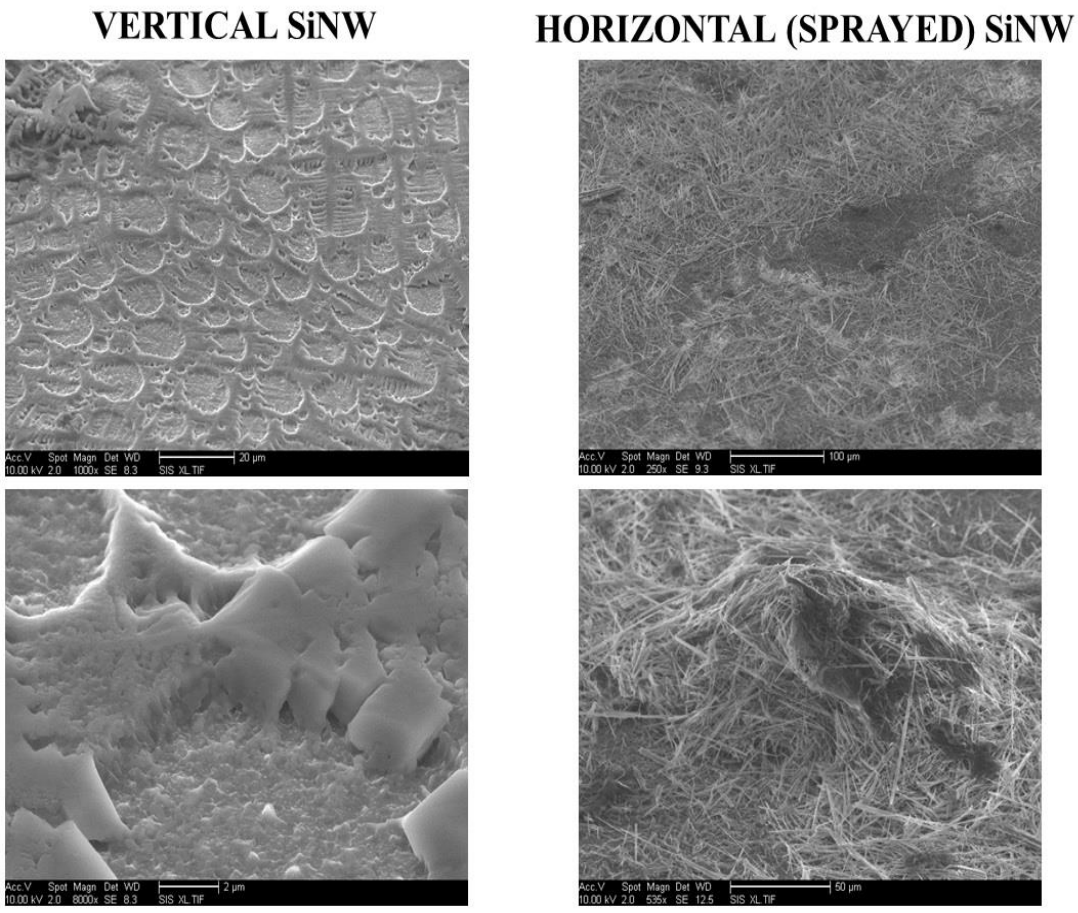

Figure 11: First noted during initial fluorescent imaging, it looked like a patterned surface not unlike a cell groove, but was too uniform to be believed as a cell groove. No such pattern was noted on horizontal array SiNW chips.

Figure 12: DIC vs. Confocal slice image comparison

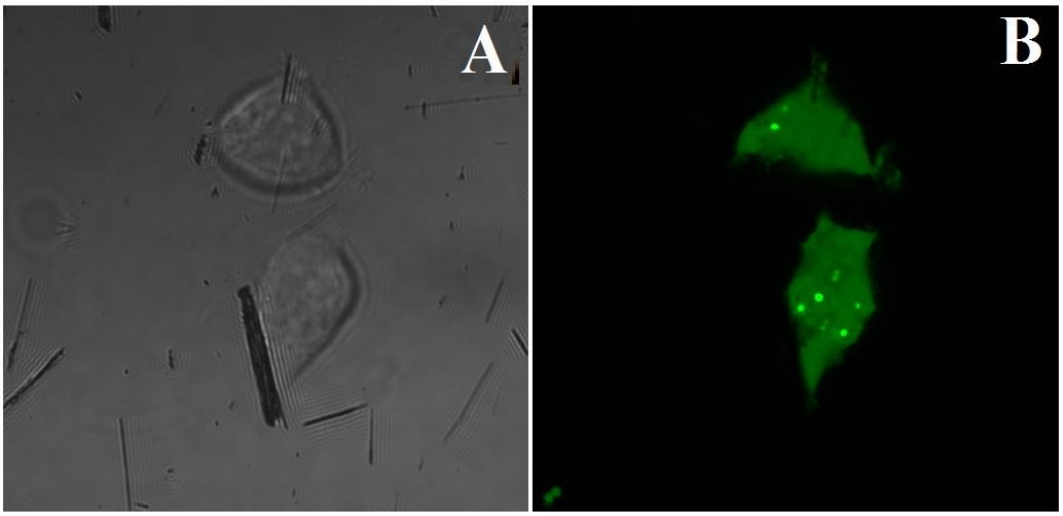

Figure 12: Figure A and B is the DIC and confocal fluorescent images of slice layer #23, respectively. Just looking at the fluorescent imaging, one may simply observe the bottom cell is unusually shaped. However, comparing with the DIC imaging it is clear the reason for its unusual shape is due to the fact it has attached itself to a bundle of NWs on one side. Upper cell shows several points of NW penetration through the cellular membrane.

Figure 13: DIC and Confocal combined image of preferential cellular adhesion to NWs

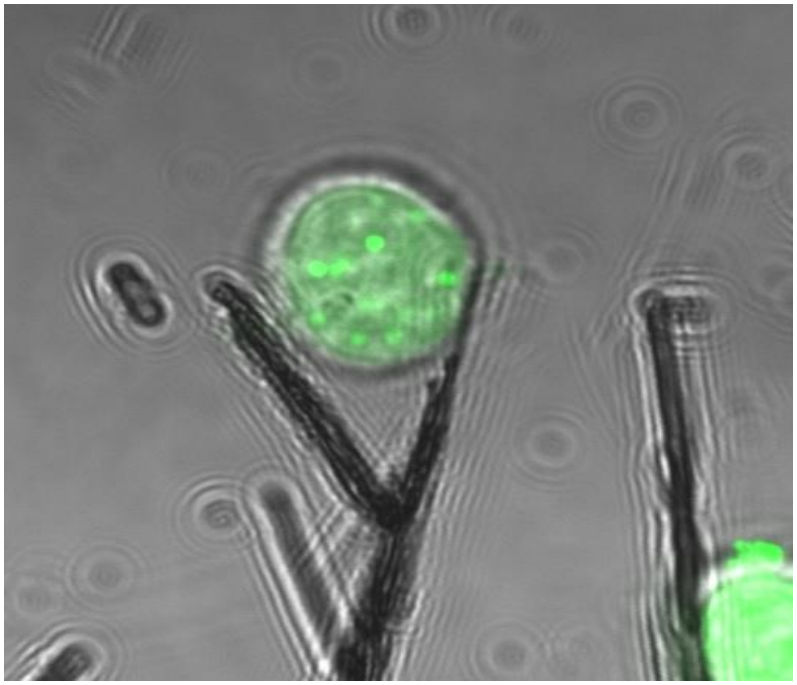

Figure 13: This figure shows combined fluorescent and DIC image of slice 17 taken with Olympus FV1000. Image shows evidence of preferential cellular adhesion to sprayed horizontal NWs. In this particular image, there are two separate cells that seem to be squeezing itself into a tree-branch like arrangement of sprayed NWs.

Figure 14: SEM image of SiNW after 30 min vs. 2 days in media without cell

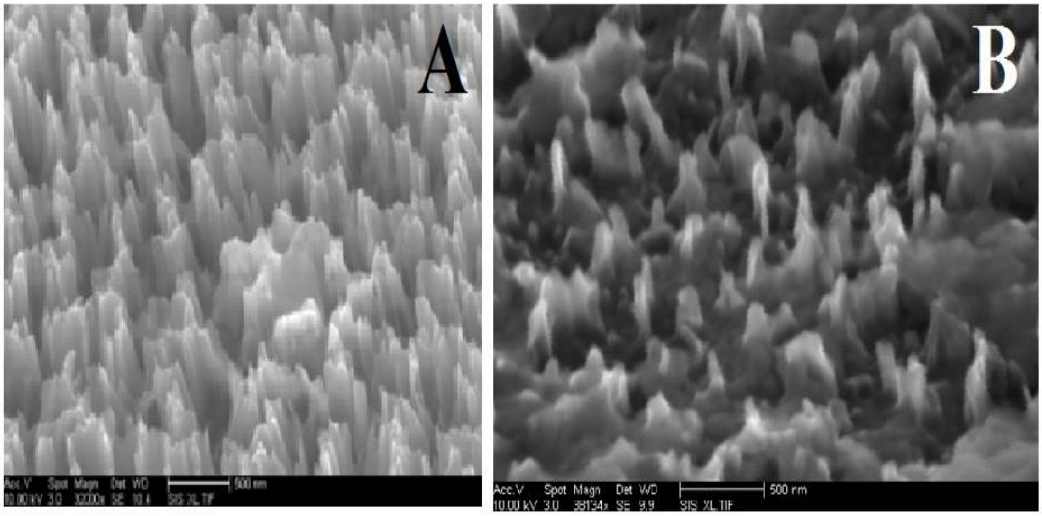

Figure 14: A) Wires after 30 mins and, B) after 2 days in culture media. The wires are shown to have vastly degenerated over the period of 2 days. The sticky materials are still found covering the top of the SiNW.

Figure 15: SEM - 2 day cell cultured with SiNW

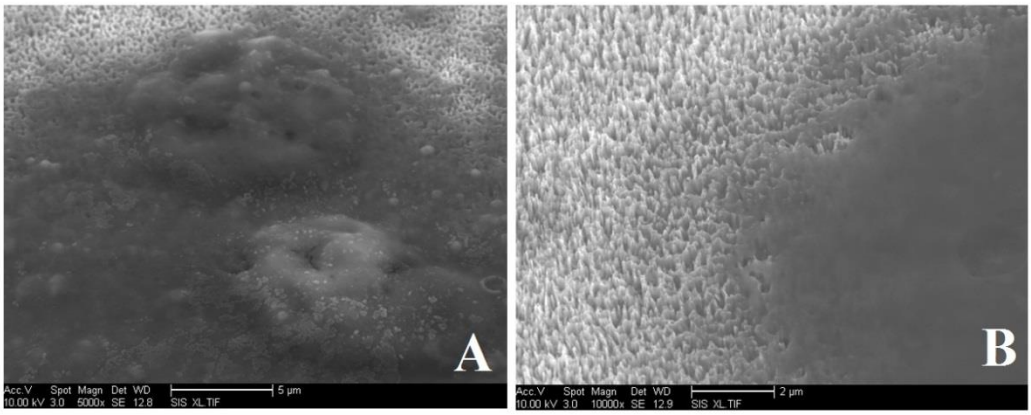

Figure 15: A) 2 Cellular structures on a bed of vertical SiNW showing higher concentration of dark sticky unknown material over the cellular body and the area around it. B) A close-up of one of the edges of where the covering material seems to be expanding. Shows clear boarder between regions of wires that are being invaded by the dark materials and the regions that are free from the coverings is seen.

Figure 16: 18 hour cell culture with SiNW

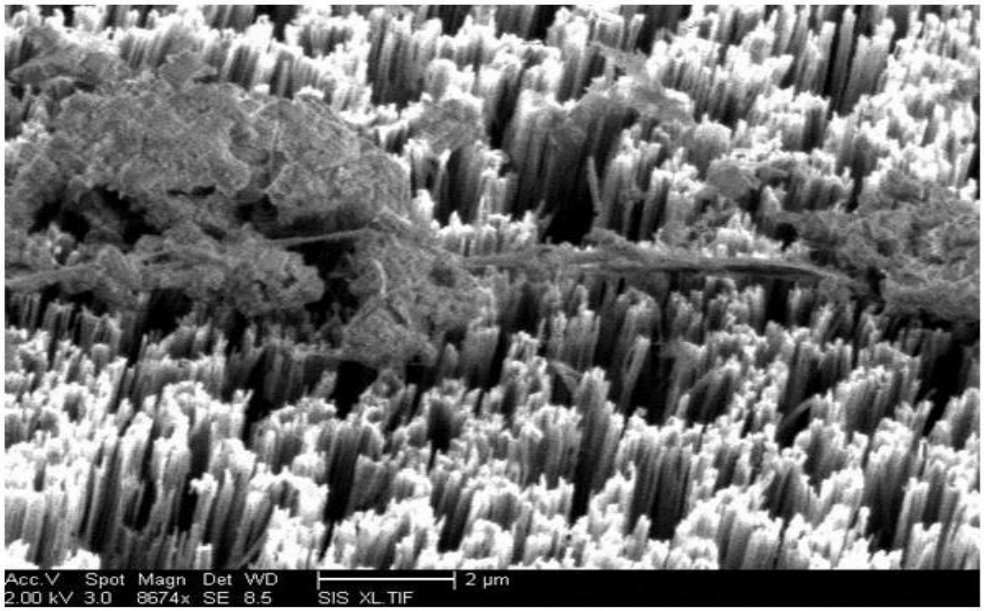

Figure 16: Healthy length of wires with moderate (some empty spots) degeneration of NWs. The cell seems to have longer processes that are reaching out to another bed of NWs.

Figure 17: NW degeneration by duration of exposure to cell culture at 5 micron scale bar

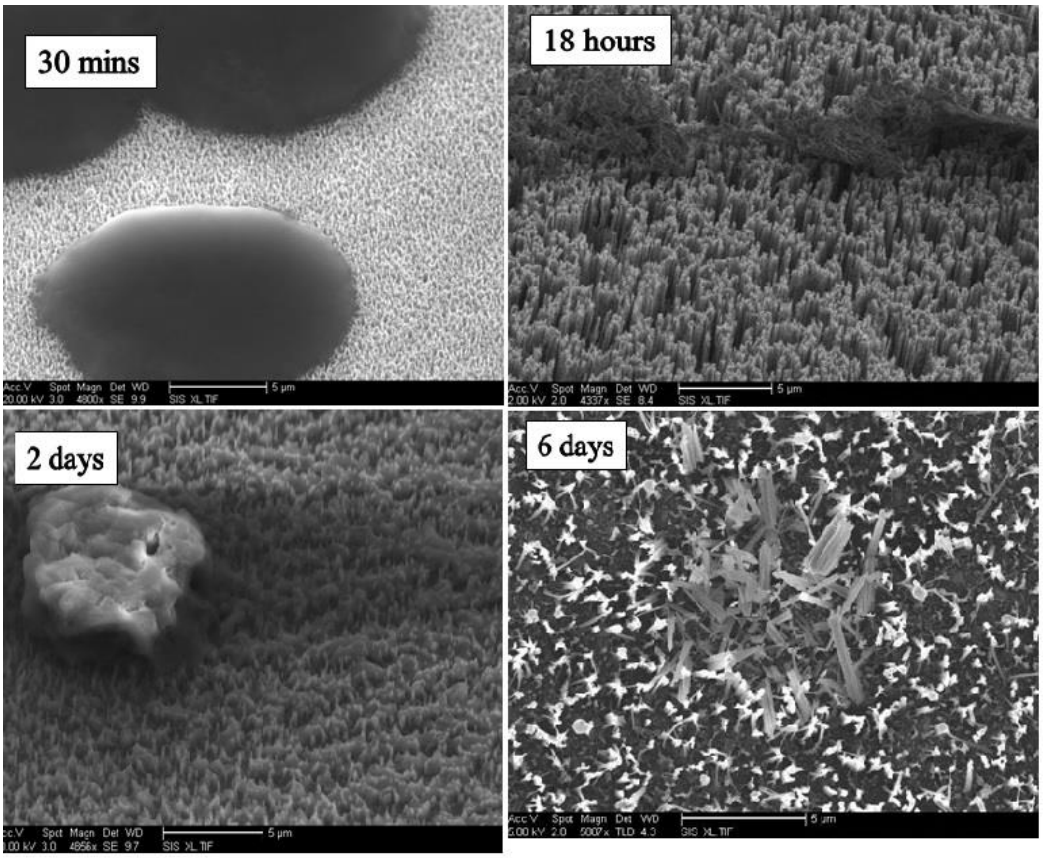

Figure 17: SEM imaging shows severe deterioration of NWs by 6 days.

Figure 18: NW degeneration by duration of exposure to cell culture at 1-2 micron scale bar

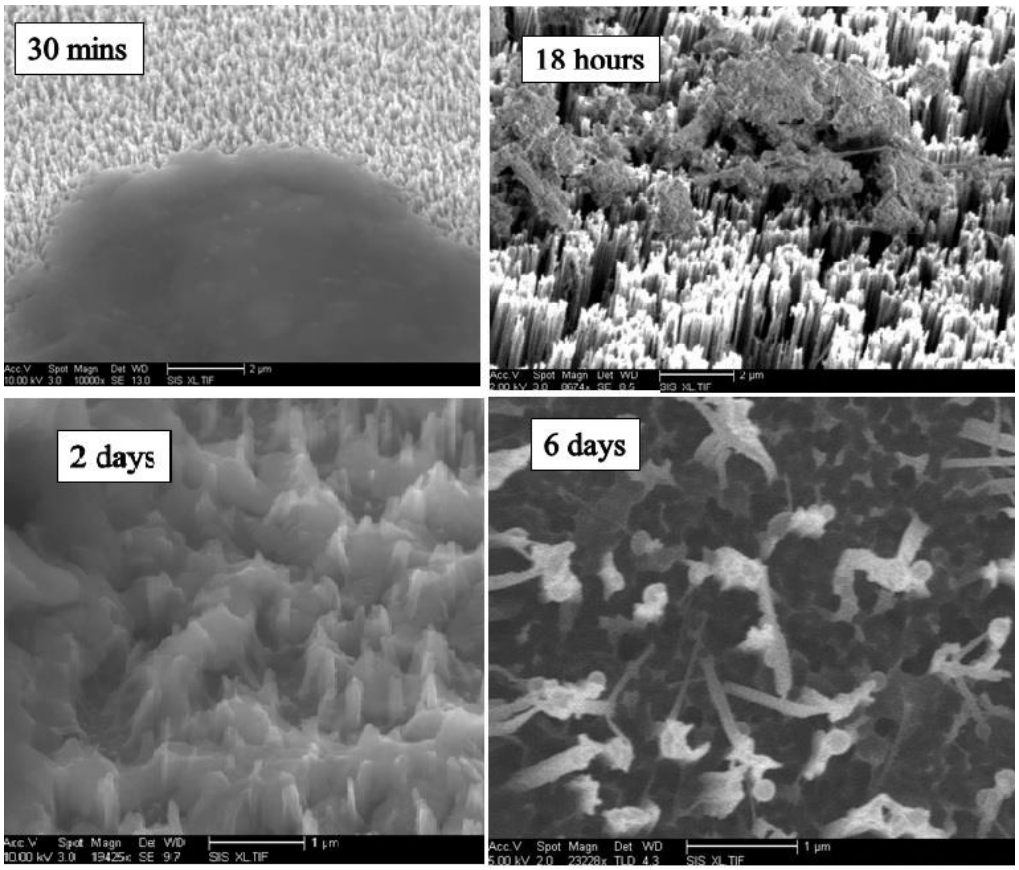

Figure 17: SEM imaging shows close-up of severe deterioration of NWs by 6 days. 30mins/18 hours scale is 2 microns; 2days/6days scale is 1 micron.

References

1. Silva, G.A. Introduction to nanotechnology and its applications to medicine. Surg Neurol. 2004 Mar;61(3):216-20.

2. Gage F, Coates PW, Palmer TD, Kuhn HG, Fisher LJ, Suhonen JO, Peterson DA, Suhr ST, Ray J. Survival and differentiation of adult neuronal progenitor cells transplanted to the adult brain. *Proc. Natl. Acad. Sci.* 92, 11879-11883 (1995).

3. Du XW, Lu YW, Kulinich SA, Sun J, Yao P. Microporous silicon connected with silicon wires. *Semicond. Sci. Tech,* 21(4), 498 (2006).

4. Peng KQ, Yan YJ, Gao SP, Zhu J. Synthesis of Large-Area Silicon Nanowire Arrays via Self-Assembling Nanoelectrochemistry. *Advanced Materials,* 14(16), 1164-1167 (2002).

5. Peng K, Yan Y, Gao S, Zhu J. Dendrite-Assisted Growth of Silicon Nanowires in Electroless Metal Deposition. *Advanced functional Materials.* 13(2), 127-132 (2003).

6. Greene LE, Yuhas BD, Law M, Zitoun D, Yang P. Solution-grown zinc oxide nanowires. *Inorg Chem* 45(19), 7535-43, (2006)

7. Tang, S., Qiu, J., Nikulina, E., Filbin, M. T. Soluble myelin-associated glycoprotein released from damaged white matter inhibits axonal regeneration. *Mol Cell Neurosci* 18, 259-269, doi:10.1006/mcne.2001.1020 S1044-7431(01)91020-6 [pii] (2001).

8. Tang, S. Woodhall RW, Shen YJ, deBellard ME, Saffell JL, Doherty P, Walsh FS, Filbin MT. Soluble myelin-associated glycoprotein (MAG) found in vivo inhibits axonal regeneration. *Mol Cell Neurosci* 9, 333-346, doi:S1044-7431(97)90633-3 [pii]10.1006/mcne.1997.0633 (1997).

9. Sivasankaran, R. Pei J, Wang KC, Zhang YP, Shields CB, XuXM, He Z. PKC mediates inhibitory effects of myelin and chondroitin sulfate proteoglycans on axonal regeneration. *Nat Neurosci* 7, 261-268, doi:10.1038/nn1193nn1193 [pii] (2004).

10. Huber, A. B. & Schwab, M. E. Nogo-A, a potent inhibitor of neurite outgrowth and regeneration. *Biol Chem* 381, 407-419, doi:10.1515/BC.2000.053 (2000).

11. Nieto-Sampedro, M. Neurite outgrowth inhibitors in gliotic tissue. *Adv Exp Med Biol* 468, 207-224 (1999).

12. Rudge, J. S. & Silver, J. Inhibition of neurite outgrowth on astroglial scars in vitro. *J Neurosci* 10, 3594-3603 (1990).

13. Chen, Z. J., Ughrin, Y. & Levine, J. M. Inhibition of axon growth by oligodendrocyte precursor cells. *Mol Cell Neurosci* 20, 125-139, doi:10.1006/mcne.2002.1102S1044743102911024 [pii] (2002).

14. Kimura-Kuroda, J. Teng X, Komuta Y, Yoshioka N, Sango K, Kawamura K, Raisman G, Kawano H. An in vitro model of the inhibition of axon growth in the lesion scar formed after central nervous system injury. *Mol Cell Neurosci* 43, 177-187, doi:S1044-7431(09)00238-3 [pii]10.1016/j.mcn.2009.10.008 (2010).

15. Yiu, G. & He, Z. Glial inhibition of CNS axon regeneration. *Nat Rev Neurosci* 7, 617-627, doi:nrn1956 [pii]10.1038/nrn1956 (2006).

16. Murray, M. & Fischer, I. Transplantation and gene therapy: combined approaches for repair of spinal cord injury. *Neuroscientist* 7, 28-41 (2001).

17. Lavdas, A. A. Chen J, Papastefanaki F, Chen S, Schachner M, Matsas R, Thomaidou D. Schwann cells engineered to express the cell adhesion molecule L1 accelerate myelination and motor recovery after spinal cord injury. *Exp Neurol* 221, 206-216, doi:S0014-4886(09)00456-7 [pii]10.1016/j.expneurol.2009.10.024 (2010).

18. Bonner, J. F., Blesch, A., Neuhuber, B. & Fischer, I. Promoting directional axon growth from neural progenitors grafted into the injured spinal cord. *J Neurosci Res* 88, 1182-1192, doi:10.1002/jnr.22288 (2010).

19. Gensel, J. C. Nakamura S, Guan Z, van Rooijen N, Ankeny DP, Popovich PG. Macrophages promote axon regeneration with concurrent neurotoxicity. *J Neurosci* 29, 3956-3968, doi:29/12/3956 [pii]10.1523/JNEUROSCI.3992-08.2009 (2009).

20. Lee, M. J. Chen CJ, Cheng CH, Huang WC, Kuo HS, Wu JC, Tsai MJ, Huang MC, Chang WC, Cheng H. Combined treatment using peripheral nerve graft and FGF-1: changes to the glial environment and differential macrophage reaction in a complete transected spinal cord. *Neurosci Lett* 433, 163-169, doi:S0304-3940(07)01226-8 [pii]10.1016/j.neulet.2007.11.067 (2008).

21. Blackmore, M. & Letourneau, P. C. Changes within maturing neurons limit axonal regeneration in the developing spinal cord. *J Neurobiol* 66, 348-360, doi:10.1002/neu.20224 (2006).

22. Davies, J. E., Huang C, Proschel C, Noble M, Mayer-Proschel M, Davies SJ. Astrocytes derived from glial-restricted precursors promote spinal cord repair. *J Biol* 5, 7, doi:jbiol35 [pii]10.1186/jbiol35 (2006).

23. Shefner, S. A. & Osmanovic, S. S. GABAA and GABAB receptors and the ionic mechanisms mediating their effects on locus coeruleus neurons. *Prog Brain Res* 88, 187-195 (1991).

24. Limozin, L. & Denet, B. Quantitative analysis of concentration gradient and ionic currents associated with hyphal tip growth in fungi. *Phys Rev E Stat Phys Plasmas Fluids Relat Interdiscip Topics* 62, 4067-4076 (2000).

25. Liu, H., Wu, M. M. & Zakon, H. H. Individual variation and hormonal modulation of a sodium channel beta subunit in the electric organ correlate with variation in a social signal. *Dev Neurobiol* 67, 1289-1304, doi:10.1002/dneu.20404 (2007).

26. Green, S. T. & Petersen, O. H. Thyroid follicular cells: the resting membrane potential and the communication network. *Pflugers Arch* 391, 119-124 (1981).

27. Koo, O. M., Rubinstein, I. & Onyuksel, H. Role of nanotechnology in targeted drug delivery and imaging: a concise review. *Nanomedicine* 1, 193-212, doi:S1549-9634(05)00123-1 [pii]10.1016/j.nano.2005.06.004 (2005).

28. Vauthier, C., Dubernet, C., Chauvierre, C., Brigger, I. & Couvreur, P. Drug delivery to resistant tumors: the potential of poly(alkyl cyanoacrylate) nanoparticles. *J Control Release* 93, 151-160, doi:S0168365903003936 [pii] (2003).

29. Peters K, Unger RE, Kirkpatrick CJ, Gatti AM, Monari E. Effects of nano-scaled particles on endothelial cell function in vitro: studies on viability, proliferation and inflammation. *Journal of Materials Science Materials in Medicine* 15(4): 321-5 (2004)